Physics Letters B 779 (2018) 201–205

Contents lists available at ScienceDirect

Physics Letters B

www.elsevier.com/locate/physletb

Scalar dark matter in leptophilic two-Higgs-doublet model

Priyotosh Bandyopadhyay [a], Eung Jin Chun [b], Rusa Mandal [c,*]

[a] Indian Institute of Technology Hyderabad, Kandi, Sangareddy-502287, Telengana, India
[b] Korea Institute for Advanced Study, Seoul 130-722, Republic of Korea
[c] The Institute of Mathematical Sciences, HBNI, Taramani, Chennai 600113, India

ARTICLE INFO

Article history:
Received 4 October 2017
Received in revised form 23 January 2018
Accepted 27 January 2018
Available online 1 February 2018
Editor: G.F. Giudice

Keywords:
Two-Higgs-doublet model
Dark matter
Direct and indirect detection

ABSTRACT

Two-Higgs-Doublet Model of Type-X in the large $\tan\beta$ limit becomes leptophilic to allow a light pseudo-scalar A and thus provides an explanation of the muon $g-2$ anomaly. Introducing a singlet scalar dark matter S in this context, one finds that two important dark matter properties, nucleonic scattering and self-annihilation, are featured separately by individual couplings of dark matter to the two Higgs doublets. While one of the two couplings is strongly constrained by direct detection experiments, the other remains free to be adjusted for the relic density mainly through the process $SS \to AA$. This leads to the 4τ final states which can be probed by galactic gamma ray detections.

1. Introduction

The existence of dark matter (DM) is supported by various astrophysical and cosmological observations in different gravitational length scales. The best candidate for dark matter is a stable neutral particle beyond the Standard Model (SM). The simplest working model is to extend the SM by adding a singlet scalar [1,2] and thus allowing its coupling to the SM Higgs doublet which determines the microscopic properties of the dark matter particle. This idea of Higgs portal has been very popular in recent years and studied extensively by many authors [3]. However, such a simplistic scenario is tightly constrained by the current direct detection experiments since a single Higgs portal coupling determines both the thermal relic density and the DM-nucleon scattering rate.

One is then tempted to study the scalar dark matter property in popular Two-Higgs-Doublet Models (2HDMs) [4]. Having more degrees of freedom, two independent Higgs portal couplings and extra Higgs bosons, one could find a large parameter space accommodating the current experimental limits and enriching phenomenological consequences [5].

The purpose of this work is to realize a scalar singlet DM through Higgs portal in the context of a specific 2HDM which can accommodate the observed deviation of the muon $g-2$. Among four types of Z_2-symmetric 2HDMs, the type-X model is found to be a unique option for the explanation of the muon $g-2$ anomaly [6] and the relevant parameter space has been explored more precisely [7–10]. Combined with the lepton universality conditions, one can find a large parameter space allowed at 2σ favoring $\tan\beta \gtrsim 30$ and $m_A \ll m_{H,H^\pm} \approx 200$–$400$ GeV [10]. The model can be tested at the LHC by searching for a light pseudo-scalar A through 4τ or $2\mu 2\tau$ final states [11–13].

In the large $\tan\beta$ regime, the SM-like Higgs boson reside mostly on the Higgs doublet with a large VEV. Therefore its coupling to DM is severely constrained by the direct detection experiments. On the other hand, the other Higgs doublet with a small VEV contains mostly the extra Higgs bosons, the light pseudo-scalar A, heavy neutral and charged bosons H and $H^\pm$, and thus its coupling to DM controls the thermal relic density preferably through the annihilation channel $SS \to AA$.

In Sec. 2, we describe the basic structure of the model. In Sec. 3 and 4, we discuss the consequences of DM-nucleon scattering and DM annihilation which determines the relic density as well as the indirect detection, respectively. We conclude in Sec. 5.

2. L2HDM with a scalar singlet

Introducing two Higgs doublets $\Phi_{1,2}$ and one singlet scalar S stabilized by the symmetry $S \to -S$, one can write down the following gauge invariant scalar potential:

$$V = m_{11}^2|\Phi_1|^2 + m_{22}^2|\Phi_2|^2 - m_{12}^2(\Phi_1^\dagger\Phi_2 + \Phi_1\Phi_2^\dagger)$$

* Corresponding author.
E-mail addresses: bpriyo@iith.ac.in (P. Bandyopadhyay), ejchun@kias.re.kr (E.J. Chun), rusam@imsc.res.in (R. Mandal).

https://doi.org/10.1016/j.physletb.2018.01.071

$$+\frac{\lambda_1}{2}|\Phi_1|^4+\frac{\lambda_2}{2}|\Phi_2|^4+\lambda_3|\Phi_1|^2|\Phi_2|^2+\lambda_4|\Phi_1^\dagger\Phi_2|^2$$
$$+\frac{\lambda_5}{2}\left[(\Phi_1^\dagger\Phi_2)^2+(\Phi_1\Phi_2^\dagger)^2\right]$$
$$+\frac{1}{2}m_0^2S^2+\frac{\lambda_S}{4}S^4+S^2\left[\kappa_1|\Phi_1|^2+\kappa_2|\Phi_2|^2\right], \quad (1)$$

where a softly-broken Z_2 symmetry is imposed in the 2HDM sector to forbid dangerous flavor violation. The model contains four more parameters compared to the usual 2HDMs: one mass parameter m_0 and three dimensionless parameters λ_S and $\kappa_{1,2}$ for the DM self-coupling and the DM-Higgs couplings, respectively. Extending the analysis in [4], one can find the following simple relations for the vacuum stability [14]:

$$\lambda_S>0,\quad \tilde{\lambda}_1>0,\quad \tilde{\lambda}_2>0,$$
$$\tilde{\lambda}_3>-\sqrt{\tilde{\lambda}_1\tilde{\lambda}_2}, \quad (2)$$
$$\tilde{\lambda}_3+\lambda_4-|\lambda_5|>-\sqrt{\tilde{\lambda}_1\tilde{\lambda}_2}$$

where $\tilde{\lambda}_1\equiv\lambda_1-\kappa_1^2/2\lambda_S$, $\tilde{\lambda}_2\equiv\lambda_2-\kappa_2^2/2\lambda_3$, and $\tilde{\lambda}_3\equiv\lambda_3-\kappa_1\kappa_2/2\lambda_S$. As we will see, the desired dark matter properties require $|\kappa_{1,2}|\ll 1$ and thus the vacuum stability condition can be easily satisfied in a large parameter space.

Minimization conditions determine the vacuum expectation values $\langle\Phi^0_{1,2}\rangle\equiv v_{1,2}/\sqrt{2}$ around which the Higgs doublets are expressed as

$$\Phi_{1,2}=\left[\eta^+_{1,2},\frac{1}{\sqrt{2}}\left(v_{1,2}+\rho_{1,2}+i\eta^0_{1,2}\right)\right]. \quad (3)$$

Removing the Goldstone modes, there appear five massive fields denoted by $H^\pm$, A, H and h. Assuming negligible CP violation, $H^\pm$ and A are given by

$$H^\pm, A=-s_\beta\,\eta_1^{\pm,0}+c_\beta\,\eta_2^{\pm,0}, \quad (4)$$

where the angle β is determined from $t_\beta\equiv\tan\beta=v_2/v_1$. The neutral CP-even Higgs bosons are diagonalized by the angle α:

$$h=-s_\alpha\rho_1+c_\alpha\rho_2,$$
$$H=+c_\alpha\rho_1+s_\alpha\rho_2, \quad (5)$$

where h denotes the lighter (125 GeV) state.

Normalizing the Yukawa couplings of the neutral bosons to a fermion f by m_f/v where $v=\sqrt{v_1^2+v_2^2}=246$ GeV, we have the following Yukawa couplings of the Higgs bosons:

$$-\mathcal{L}_Y=\sum_{f=u,d,\ell}\frac{m_f}{v}\left(y_f^h h\bar{f}f+y_f^H H\bar{f}f-iy_f^A A\bar{f}\gamma_5 f\right)$$
$$+\left[\sqrt{2}V_{ud}H^+\bar{u}\left(\frac{m_u}{v}y_u^A P_L+\frac{m_d}{v}y_d^A P_R\right)d\right.$$
$$\left.+\sqrt{2}\frac{m_l}{v}y_\ell^A H^+\bar{\nu}P_R\ell+\text{h.c.}\right]. \quad (6)$$

Recall that the type-X 2HDM assigns the Z_2 symmetry under which Φ_1 and right-handed leptons are odd; and the other particles are even, and thus Φ_2 couples to all the quarks and Φ_1 to leptons.

As a consequence, one has the normalized Yukawa couplings $y_f^{h,H,A}$ given by

$y^A_{u,d}$	y^A_ℓ	$y^H_{u,d}$	y^H_ℓ	$y^h_{u,d}$	y^h_ℓ
$\pm\frac{1}{t_\beta}$	t_β	$\frac{s_\alpha}{s_\beta}$	$\frac{c_\alpha}{c_\beta}$	$\frac{c_\alpha}{s_\beta}$	$-\frac{s_\alpha}{c_\beta}$

(7)

As the 125 GeV Higgs (h) behaves like the SM Higgs boson, we can safely take the alignment limit of $\cos(\beta-\alpha)\approx 0$ and $|y_f^h|\approx 1$ and $y_{u,d}^{A,H}\propto 1/t_\beta$ and $y_l^{A,H}\propto t_\beta$. Notice that A and H couple dominantly to the tau in the large $\tan\beta$ limit.

The singlet and doublet scalar couplings are given by

$$V=\frac{1}{2}S^2\left[2v(\kappa_h h+\kappa_H H)+\kappa_{hh}h^2+2\kappa_{hH}hH\right.$$
$$\left.+\kappa_{HH}H^2+\kappa_{AA}(A^2+2H^+H^-)\right],$$
$$\text{where}\quad \kappa_h=-\kappa_1 s_\alpha c_\beta+\kappa_2 c_\alpha s_\beta\approx\kappa_1 c_\beta^2+\kappa_2 s_\beta^2,$$
$$\kappa_H=+\kappa_1 c_\alpha c_\beta+\kappa_2 s_\alpha s_\beta\approx(\kappa_1-\kappa_2)c_\beta s_\beta.$$
$$\kappa_{hh}=\kappa_1 s_\alpha^2+\kappa_2 c_\alpha^2\approx\kappa_1 c_\beta^2+\kappa_2 s_\beta^2,$$
$$\kappa_{hH}=-(\kappa_1-\kappa_2)c_\alpha s_\alpha\approx(\kappa_1-\kappa_2)c_\beta s_\beta,$$
$$\kappa_{HH}=\kappa_1 c_\alpha^2+\kappa_2 s_\alpha^2\approx\kappa_1 s_\beta^2+\kappa_2 c_\beta^2,$$
$$\kappa_{AA}=\kappa_1 s_\beta^2+\kappa_2 c_\beta^2, \quad (8)$$

which shows interesting relations in the alignment limit: $\kappa_h\approx\kappa_{hh}$, $\kappa_H\approx\kappa_{hH}$, and $\kappa_{HH}\approx\kappa_{AA}$. Furthermore, one finds further simplification: $\kappa_{h,hh}\sim\kappa_2$, $\kappa_{H,hH}\sim 0$, and $\kappa_{AA,HH}\sim\kappa_1$ neglecting small contributions suppressed by $1/t_\beta$. This behavior determines the major characteristic of the model.

Before starting our main discussions, let us make a few comments on the LHC probe of the model. As shown in Eq. (7), the extra Higgs couplings to quarks are proportional to $1/t_\beta$ and thus their single production is suppressed by $1/t_\beta^2$ compared to the SM Higgs production. For this reason a light A (and H) is still allowed by the direct search of di-tau final state at ATLAS [15] in the large $\tan\beta$ limit, which also explains the muon $g-2$ anomaly. One can also look for usual electroweak productions of $pp\to HA, H^\pm A$, ending up with multi-tau signals [11], or the SM Higgs production and its exotic decay $h\to AA$ [13]. The $pp\to HA$ process is of particular interest in the model under consideration as it could lead to a promising signature of di-tau associated with large missing energy. Having $\kappa_H\propto 1/t_\beta$, however, the $H\to SS$ process (when allowed kinematically) is highly suppressed in the large $\tan\beta$ limit and thus hardly be probed at the LHC. The recent bounds on the multi-tau events searched by ATLAS in the case of the chargino/neutralino production [16] could be relevant for our model parameter space. Applying the same cuts, e.g., $\not{p}_T>150$ GeV and $p_T^{\tau_1,\tau_2}>50,40$ GeV, to our processes, we find that no events survive for the final states searched in Ref. [16]. This is basically due to the following differences: (i) the $H^\pm A$ and HA production cross-sections are smaller than the chargino/neutralino production by almost one order of magnitude; (ii) our processes do not generate large missing energy, and τ's coming from a light A become too soft to pass the above hard cuts as indicated in Ref. [11]. We have also checked the recent bounds on $2\ell/3\ell+\not{p}_T$ final states with kinematic demands: $p_T^\ell\geq 20,30$ GeV and $\not{p}_T\geq 130,150$ GeV, etc. [17]. However, in the given parameter space we have the following branching fraction $\mathcal{B}(H\to AZ)\sim 68\%$, $\mathcal{B}(H\to\tau\tau)\sim 32\%$ and $\mathcal{B}(A\to\tau\tau)\sim 99\%$. The charged Higgs also dominantly decays to $AW^\pm$ ($\sim 70\%$), which makes all the dominant production modes, i.e. HA, $HH^\pm$ and $H^\pm A$, insensitive to the search of multi-lepton plus large missing energy final states. Thus the recent bounds on the multi-lepton plus missing energy events motivated to probe supersymmetric signals [17] can easily be evaded.

3. DM-nucleon scattering

The spin-independent (SI) nucleonic cross section of the DM is given by

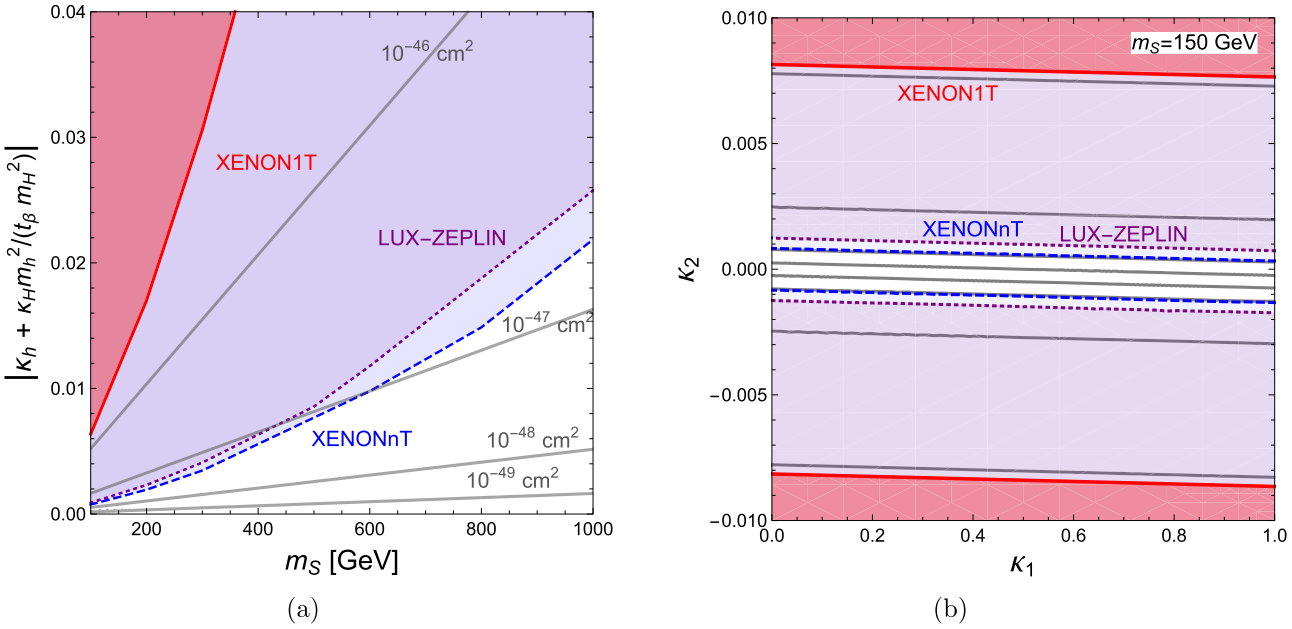

Fig. 1. (a) The allowed parameter space in the DM mass m_S and the combination of couplings plane for SI scattering cross section. The red solid curve is the current bound from XENON1T [19] experiment and the purple dot and blue dashed curves are the expected bounds in LUX-ZEPLIN [20] and XENONnT [21] experiments, respectively. The region above the mentioned curves are excluded at 90% confidence level. (b) The allowed region in $\kappa_1 - \kappa_2$ plane is illustrated by choosing $m_S = 150$ GeV from the left panel figure. The color code is the same as of the left panel. We take $m_H = 250$ GeV and $t_\beta = 50$ for these plots. (For interpretation of the references to color in this figure legend, the reader is referred to the web version of this article.)

$$\sigma_N = \frac{m_N^2 v^2}{\pi (m_S + m_N)^2} \left(\frac{\kappa_h g_{NNh}}{m_h^2} + \frac{\kappa_H g_{NNH}}{m_H^2} \right)^2 , \tag{9}$$

where $g_{NNh} \approx 0.0011$ [18] and $g_{NNH} \approx g_{NNh}/t_\beta$.

In Fig. 1(a), by considering the latest XENON1T bound [19] (red solid) and the future sensitivity of the two experiments LUX-ZEPLIN [20] (purple dotted) and XENONnT [21] (blue dashed), we highlight the allowed region in the plane of DM mass m_S and the combination of couplings $\left|\kappa_h + \frac{\kappa_H}{t_\beta}\frac{m_h^2}{m_H^2}\right|$. The shaded region above the mentioned direct detection experiment bounds are excluded at 90% confidence level. For further illustration, in Fig. 1(b), we choose a benchmark point $m_S = 150$ GeV and show the allowed parameter space in $\kappa_1 - \kappa_2$ plane for $m_H = 250$ GeV and $t_\beta = 50$. The color code is the same as in Fig. 1(a). Note that in the limit of $t_\beta \gg 1$ and $m_H > m_h$, the combined coupling is dominated simply by κ_2 and thus strongly constrained as in the SM Higgs portal scenario. One can also see that it is not possible to make the combined coupling small through cancellation between two large couplings. The other coupling κ_1 is rather unconstrained and thus this freedom allows us to reproduce the right relic density of dark matter.

4. DM annihilation

In our scenario with $m_A < m_h < m_{H,H^\pm}$ and $t_\beta \gtrsim 30$, one can read from the DM couplings (8) that the main DM annihilation channels depending on m_S can be categorized simply by $SS \to \tau\bar{\tau}$ for $m_S < m_A$; $SS \to AA$ for $m_S > m_A$, and $SS \to AA, HH/H^+H^-$ for $m_S > m_{H,H^\pm}$. For our analysis, we take a representative parameter set: $m_A = 50$ GeV, $m_{H,H^\pm} = 250$ GeV, and $t_\beta = 50$.

First, in case of $m_S < m_A$, the DM pair annihilation goes through $SS \to h^*/H^* \to \tau\bar{\tau}$, leading to the corresponding annihilation rate:

$$\sigma v_{rel}(SS \to \tau\bar{\tau}) = \frac{m_\tau^2}{4\pi} \left| \frac{\kappa_h}{P_h} + \frac{\kappa_H t_\beta}{P_H} \right|^2 \left(1 - \frac{m_\tau^2}{m_S^2}\right)^{3/2} , \tag{10}$$

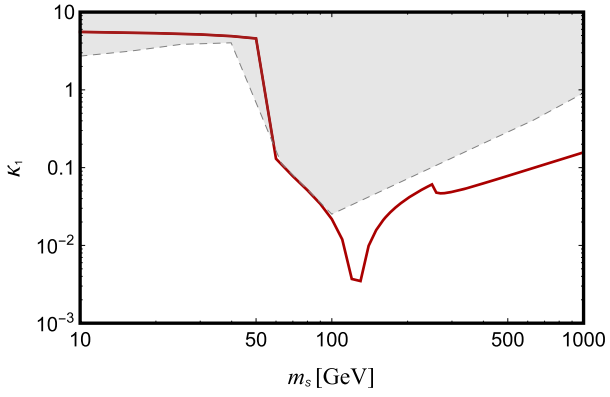

Fig. 2. The right DM relic density is obtained by the red line through the DM annihilation channels $SS \to \tau\tau$, AA, and HH/H^+H^-. The gray shaded region is excluded by Fermi-LAT gamma ray detection in the 2τ [22] and 4τ [23] final states. The plot is obtained for $m_A = 50$ GeV, $m_{H,H^\pm} = 250$ GeV, and $t_\beta = 50$. (For interpretation of the references to color in this figure legend, the reader is referred to the web version of this article.)

where $P_{h,H} \equiv 4m_S^2 - m_{h,H}^2 + i\Gamma_{h,H} m_{h,H}$. Away from the resonance point, the thermal freeze-out condition, $\sigma v_{rel} \approx 2 \times 10^{-9}$ GeV^{-2}, is satisfied by

$$\left|\kappa_h + \kappa_H t_\beta \frac{m_h^2}{m_H^2}\right| \approx 1.45 . \tag{11}$$

Considering the required limit of $\kappa_1 \gg \kappa_2$ (and thus $\kappa_H \approx \kappa_1/t_\beta$), Eq. (11) requires

$$|\kappa_1| \approx 5.8 \left(\frac{m_H}{250\,\text{GeV}}\right)^2 . \tag{12}$$

This behavior is shown by the red curve for $m_S < 50$ GeV in Fig. 2, which is however disfavored by the recent Fermi-LAT detection of gamma rays from dwarf galaxies [22].

For $m_S > m_A$, the $SS \to AA$ channel is the dominant annihilation process leading to

$$\sigma v_{rel}(SS \to AA) = \frac{1}{16\pi m_S^2}\sqrt{1-\frac{m_A^2}{m_S^2}} \times \left(\kappa_{AA} + \frac{\kappa_h \lambda_{hAA}\, v^2(4m_S^2 - m_h^2)}{|P_h|^2} + \frac{\kappa_H \lambda_{HAA}\, v^2(4m_S^2 - m_H^2)}{|P_H|^2}\right)^2, \quad (13)$$

where in the alignment limit the triple scalar couplings are given by

$$\lambda_{hAA} = \frac{\left(m_h^2 - 2m_A^2\right)\left(c_\beta^2 - s_\beta^2\right)}{v^2}, \quad (14)$$

$$\lambda_{HAA} = \frac{1}{v^2}\left[m_H^2 s_\beta^2\left(1+t_\beta\right) - m_{12}^2\left(\frac{1}{c_\beta^2} + \frac{1}{s_\beta^2}\right) + 4m_A^2 c_\beta s_\beta\right]. \quad (15)$$

The curve satisfying relic density with the mentioned annihilation mode can be seen from Fig. 2 for the range $50\,\text{GeV} < m_S < 250\,\text{GeV}$. As discussed in Sec. 2 that in the large t_β limit $\kappa_h \simeq \kappa_2$, the resonance behavior at $m_S = m_h/2$ is absent in $m_S - \kappa_1$ plane. It can also be seen that due to $\lambda_{HAA} > \lambda_{hAA}$, a huge enhancement of annihilation cross section near the H resonance region rendering tiny values of κ_1 to obtain the observed relic density.

For $m_S > m_{H,H^\pm}$, the $SS \to HH, H^+H^-$ channels are open to give additional contribution given as

$$\sigma v_{rel}(SS \to HH/H^+H^-) = \frac{3}{16\pi m_S^2}\sqrt{1-\frac{m_H^2}{m_S^2}} \times \left(\kappa_{AA} + \frac{\kappa_h \lambda_{hH^+H^-}\, v^2(4m_S^2 - m_h^2)}{|P_h|^2} + \frac{\kappa_H \lambda_{HH^+H^-}\, v^2(4m_S^2 - m_H^2)}{|P_H|^2}\right)^2, \quad (16)$$

assuming $m_H = m_{H^\pm}$. The triple scalar couplings at the alignment limit are

$$\lambda_{hH^+H^-} = \frac{\left(m_h^2 - 2m_H^2\right)\left(c_\beta^2 - s_\beta^2\right)}{v^2}, \quad (17)$$

$$\lambda_{HH^+H^-} = \frac{1}{v^2}\left[m_H^2 s_\beta^2\left(1+t_\beta + \frac{4}{c_\beta}\right) - m_{12}^2\left(\frac{1}{c_\beta^2} + \frac{1}{s_\beta^2}\right)\right]. \quad (18)$$

The total effect of all three annihilation channels namely $SS \to \tau\tau$, AA, HH/H^+H^- in the analysis is depicted in Fig. 2 for the range $m_S > 250\,\text{GeV}$ where the observed relic density is easily obtainable with $\kappa_1 \simeq \mathcal{O}(10^{-1})$.

Fermi-LAT gamma ray detection from dwarf galaxies put strong bounds on the annihilation rates for the 2τ (Fig. 1 in Ref. [22]) and 4τ (Fig. 9 in Ref. [23]) final states. Both of them are similar, disfavoring $m_S \lesssim 80$ GeV. In Fig. 2, we show the excluded parameter space in gray shaded region. It should be noted that the indirect bound shown here is imposed in a conservative way assuming 100% branching fraction for H and $H^\pm$ to τ states and still leaves the region $m_S \geq 80\,\text{GeV}$ completely accessible. In principle, one has to consider the decay channels $H \to AZ$ and $H^\pm \to AW^\pm$ leading to one more step for the tau productions. However, it does not put a meaningful bound for $m_S > m_{H,H^\pm}$ as it slightly modifies the gamma ray bound which can be found from Fig. 9 of Ref. [23].

5. Conclusion

In this work we consider an extension of the SM with an additional $SU(2)_L$ Higgs doublet and with a singlet scalar serving as a viable DM candidate. Our particular interest is in the 2HDM of Type-X which can explain muon $g-2$ anomaly in the parameter space allowing a light pseudo-scalar A and large $\tan\beta$, and thus provides interesting testable signatures at the LHC. This scenario reveals a simple characteristic of the allowed parameter space consistent with the observed DM relic density and various constraints from direct and indirect detections.

The strong constraint on the SM Higgs portal scenario from direct detection experiments is evaded in a distinguishing way by extra Higgs portal present in the model. The recent XENON1T limit and the future sensitivity of XENONnT and LUX-ZEPLIN experiments severely constrains the quartic coupling κ_2 of the DM to one of the Higgs doublets (mostly SM-like) whereas the coupling κ_1 to other Higgs doublet is permitted up to $\mathcal{O}(1)$ values.

Such freedom allows us to obtain the correct relic density in the parameter space where muon $g-2$ anomaly can be explained. In this region of parameter space, the relevant annihilation channels for the DM pair are $\tau\tau$, AA, HH/H^+H^-. As the DM annihilation leads to the 2τ or 4τ final state, Fermi-LAT data from gamma ray detection exclude the DM mass below about 80 GeV. We find that the relic density can be obtained with reasonable values of the coupling κ_1 for the DM mass opening up the annihilation channel of AA.

Acknowledgements

EJC thanks the Galileo Galilei Institute for Theoretical Physics (GGI) for the hospitality and discussions within the program “Collider Physics and the Cosmos”.

References

[1] V. Silveira, A. Zee, Phys. Lett. B 161 (1985) 136.
[2] J. McDonald, Phys. Rev. D 50 (1994) 3637.
[3] For a recent update and a comprehensive list of references, see, P. Athron, et al., GAMBIT Collaboration, Eur. Phys. J. C 77 (8) (2017) 568.
[4] J.F. Gunion, H.E. Haber, Phys. Rev. D 67 (2003) 075019.
[5] C. Bird, R.V. Kowalewski, M. Pospelov, Mod. Phys. Lett. A 21 (2006) 457;
X.G. He, T. Li, X.Q. Li, H.C. Tsai, Mod. Phys. Lett. A 22 (2007) 2121;
B. Grzadkowski, P. Osland, Phys. Rev. D 82 (2010) 125026;
M. Aoki, S. Kanemura, O. Seto, Phys. Lett. B 685 (2010) 313;
T. Li, Q. Shafi, Phys. Rev. D 83 (2011) 095017;
M.S. Boucenna, S. Profumo, Phys. Rev. D 84 (2011) 055011;
Y. Bai, V. Barger, L.L. Everett, G. Shaughnessy, Phys. Rev. D 88 (2013) 015008;
L. Wang, X.F. Han, Phys. Lett. B 739 (2014) 416;
A. Drozd, B. Grzadkowski, J.F. Gunion, Y. Jiang, J. High Energy Phys. 1411 (2014) 105;
N. Okada, O. Seto, Phys. Rev. D 90 (8) (2014) 083523;
R. Campbell, S. Godfrey, H.E. Logan, A.D. Peterson, A. Poulin, Phys. Rev. D 92 (5) (2015) 055031;
A. Hektor, K. Kannike, L. Marzola, J. Cosmol. Astropart. Phys. 1510 (10) (2015) 025;
A. Drozd, B. Grzadkowski, J.F. Gunion, Y. Jiang, J. Cosmol. Astropart. Phys. 1610 (10) (2016) 040;
X.G. He, J. Tandean, J. High Energy Phys. 1612 (2016) 074.
[6] A. Broggio, E.J. Chun, M. Passera, K.M. Patel, S.K. Vempati, J. High Energy Phys. 1411 (2014) 058.
[7] J. Cao, P. Wan, L. Wu, J.M. Yang, Phys. Rev. D 80 (2009) 071701.
[8] L. Wang, X.F. Han, J. High Energy Phys. 1505 (2015) 039.
[9] T. Abe, R. Sato, K. Yagyu, J. High Energy Phys. 1507 (2015) 064.

[10] E.J. Chun, J. Kim, J. High Energy Phys. 1607 (2016) 110.
[11] E.J. Chun, Z. Kang, M. Takeuchi, Y.L.S. Tsai, J. High Energy Phys. 1511 (2015) 099.
[12] D. Goncalves, D. Lopez-Val, Phys. Rev. D 94 (9) (2016) 095005.
[13] E.J. Chun, S. Dwivedi, T. Mondal, B. Mukhopadhyaya, arXiv:1707.07928 [hep-ph].
[14] K.G. Klimenko, Theor. Math. Phys. 62 (1985) 58, Teor. Mat. Fiz. 62 (1985) 87.
[15] M. Aaboud, et al., ATLAS Collaboration, arXiv:1709.07242 [hep-ex].
[16] M. Aaboud, et al., ATLAS Collaboration, arXiv:1708.07875 [hep-ex].
[17] ATLAS Collaboration, Tech. Rep. ATLAS-CONF-2017-039, CERN, Geneva, Jun 2017.
[18] J.M. Alarcon, J. Martin Camalich, J.A. Oller, Phys. Rev. D 85 (2012) 051503; J.M. Alarcon, L.S. Geng, J. Martin Camalich, J.A. Oller, Phys. Lett. B 730 (2014) 342.
[19] E. Aprile, et al., XENON Collaboration, arXiv:1705.06655 [astro-ph.CO].
[20] B.J. Mount, et al., arXiv:1703.09144 [physics.ins-det].
[21] E. Aprile, et al., XENON Collaboration, J. Cosmol. Astropart. Phys. 1604 (04) (2016) 027.
[22] M. Ackermann, et al., Fermi-LAT Collaboration, Phys. Rev. Lett. 115 (23) (2015) 231301.
[23] G. Elor, N.L. Rodd, T.R. Slatyer, W. Xue, J. Cosmol. Astropart. Phys. 1606 (06) (2016) 024.